Supporting Information

Förster resonance energy transfer in fluorophore labeled poly(2-ethyl-2-oxazoline)s

Ronald Merckx[a], Thomas Swift[b], Ryan Rees[b], Joachim F. R. Van Guyse[a], Ella Schoolaert[c], Karen De Clerck[c], Heidi Ottevaere[d], Hugo Thienpont[d], Valentin Victor Jerca[a,e], Richard Hoogenboom[a]**

[a]Supramolecular Chemistry Group, Centre of Macromolecular Chemistry (CMaC), Department of Organic and Macromolecular Chemistry, Ghent University, Krijgslaan 281-S4, 9000 Ghent, Belgium

[b]Polymer and Biomaterials Chemistry Laboratories, School of Chemistry and Biosciences, University of Bradford, Bradford BD7 1DP, UK

[c]Centre for Textile Science and Engineering, Department of Materials, Textiles and Chemical Technology, Ghent University, Tech Lane Science Park 70A, 9052 Ghent, Belgium

[d]Brussels Photonics (B-PHOT) – Department of Applied Physics and Photonics, Vrije Universiteit Brussel, Pleinlaan 2, 1050 Brussels, Belgium

[e]Centre of Organic Chemistry "Costin D. Nenitzescu" Romanian Academy, Spl. Independentei 202B, 060023, Bucharest, Romania

Table of contents

S1: Characterization of single and dual fluorescent dye labeled PEtOx polymers

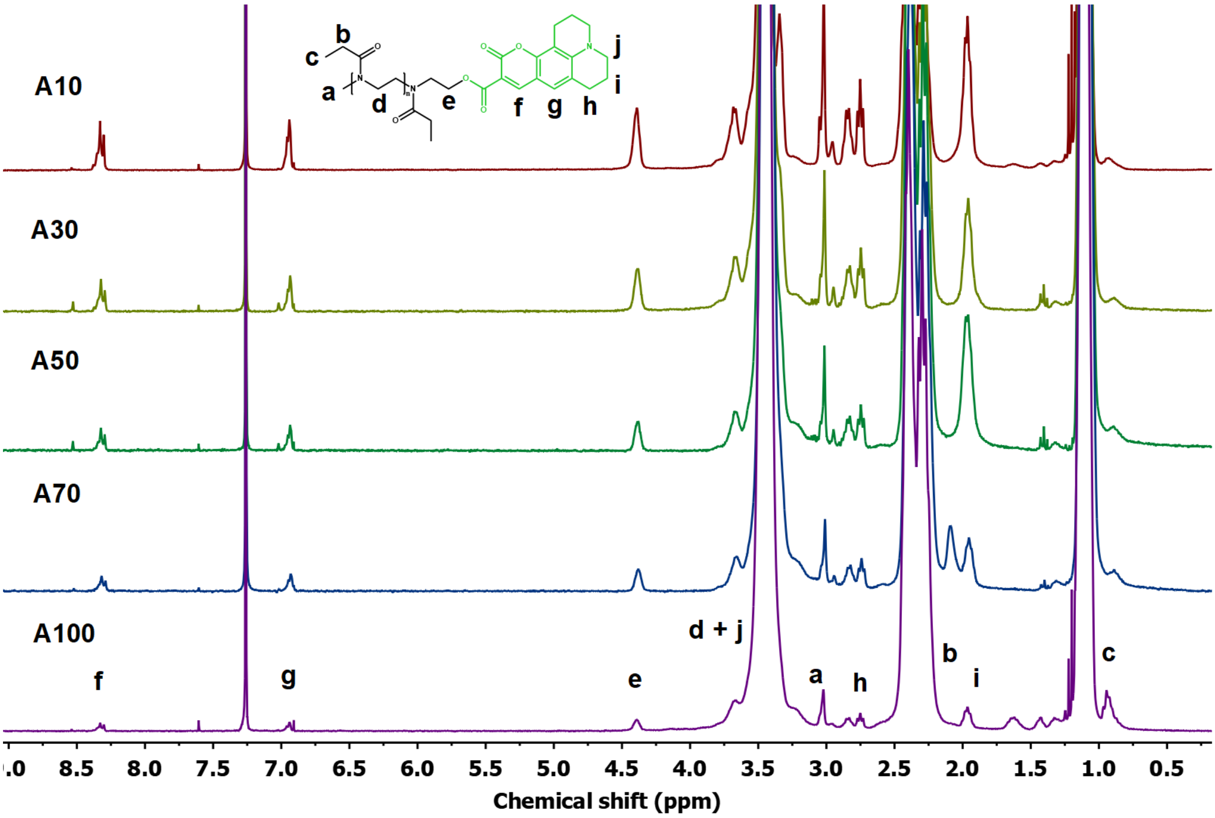

Figure S1. [1]H-NMR spectra of ω-coumarin 343 single labeled PEtOx polymers (A10-A100).

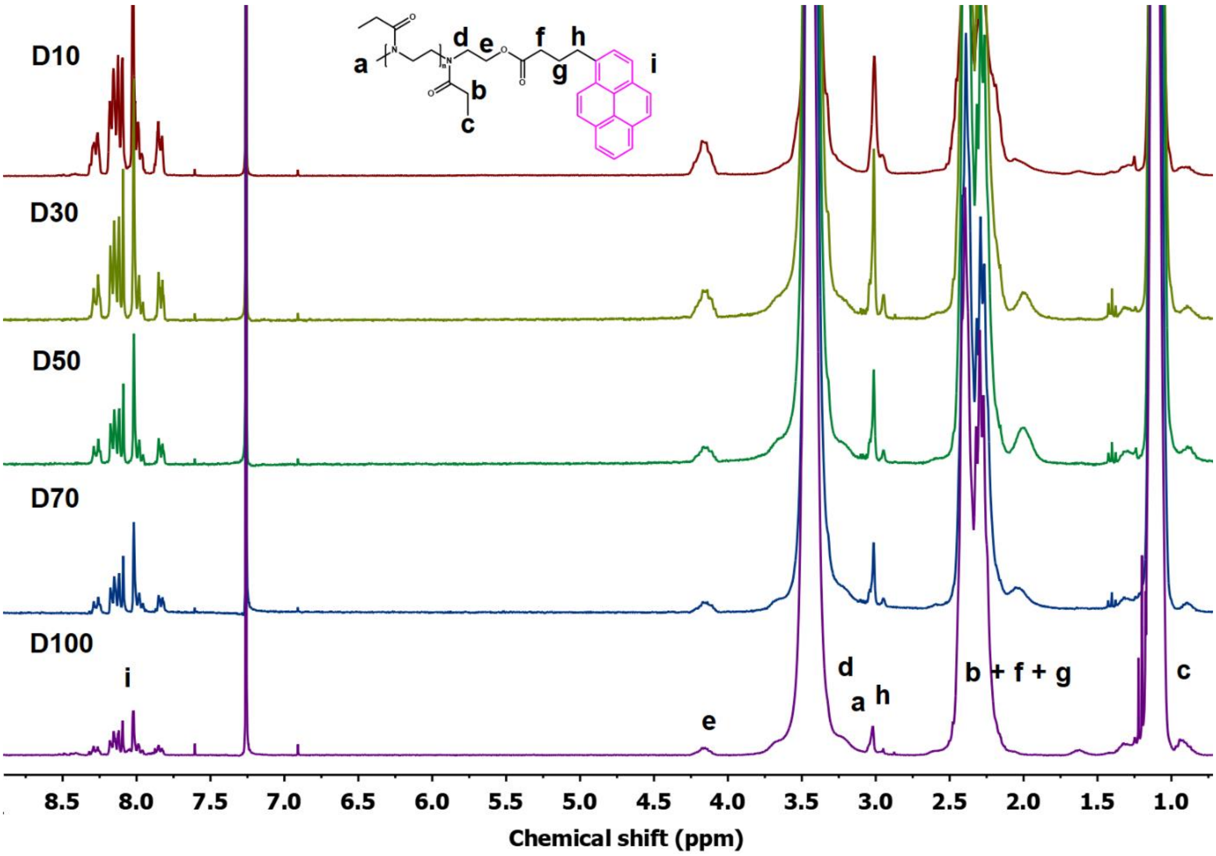

Figure S2. [1]H-NMR spectra of ω-pyrene single labeled PEtOx polymers (D10-D100).

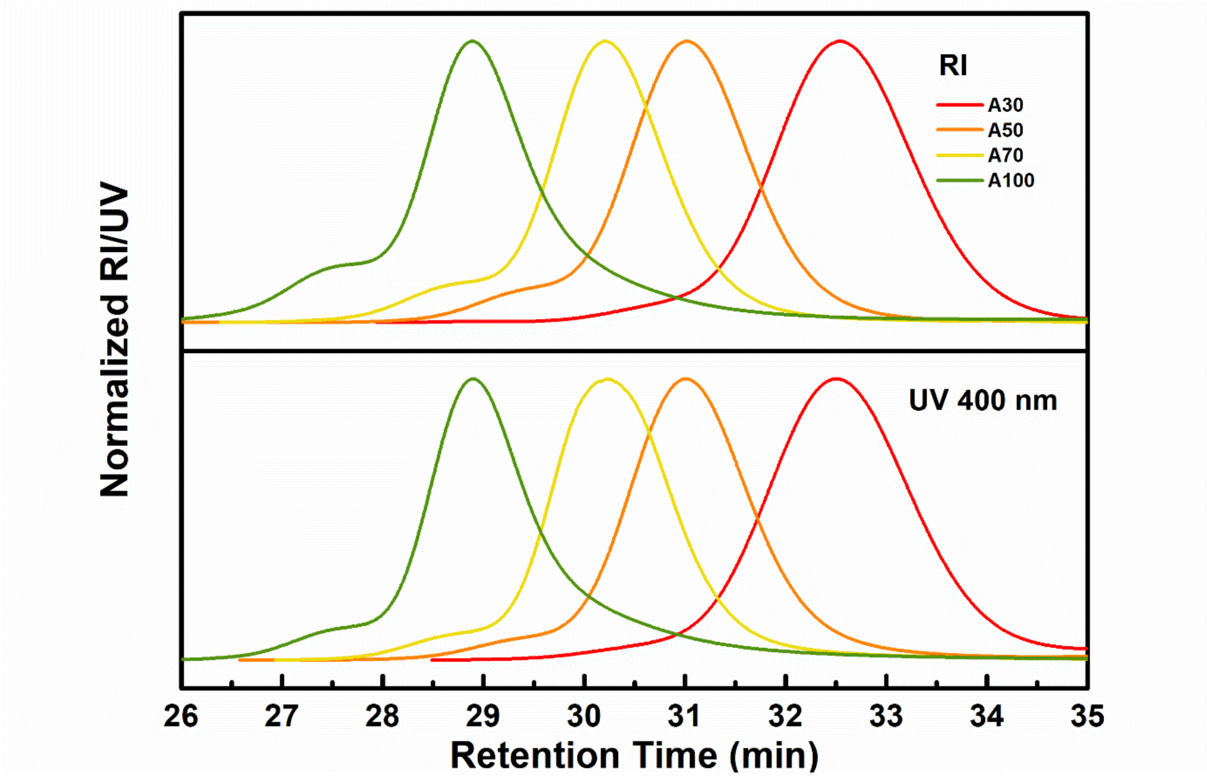

Figure S3. Normalized SEC-RI (top) and SEC UV (bottom) traces of coumarin 343 single labeled PEtOx polymers (A30-A100).

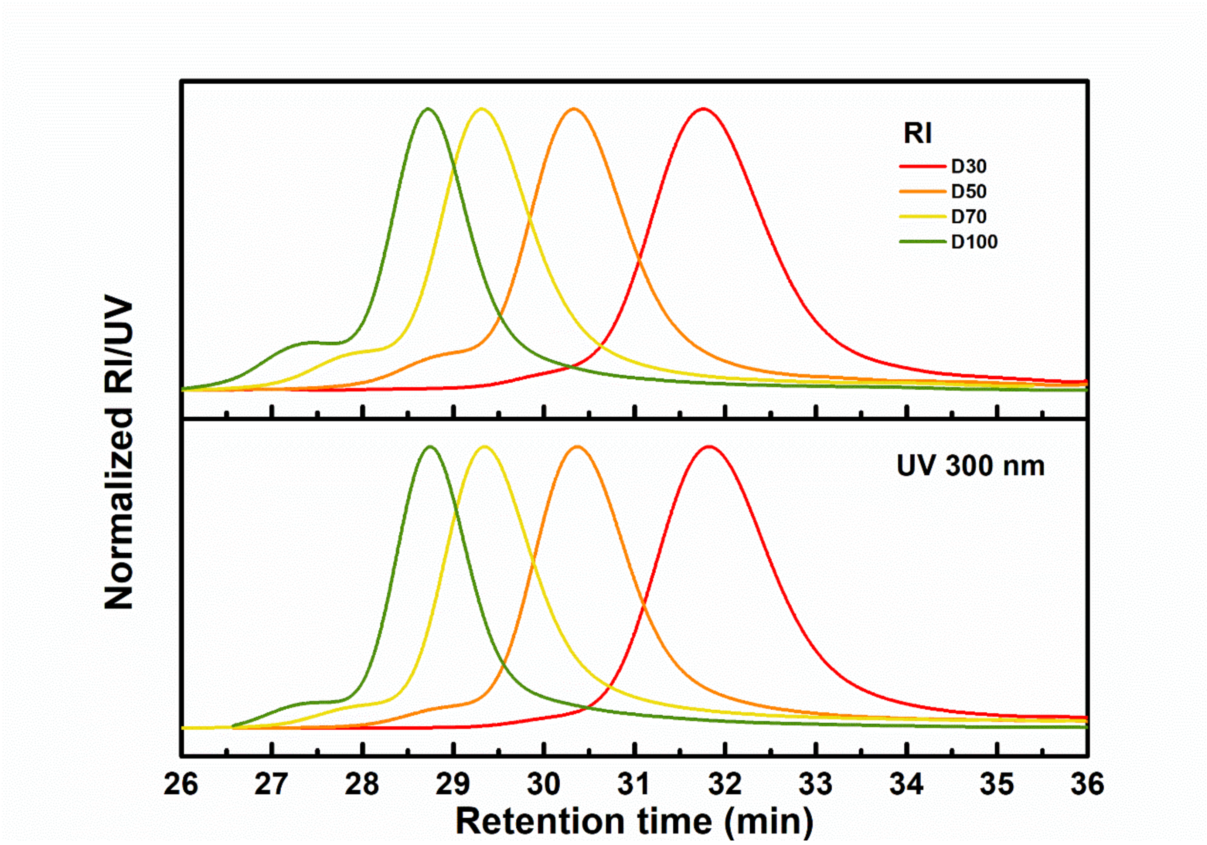

Figure S4. Normalized SEC-RI (top) and SEC UV (bottom) traces of pyrene single labeled PEtOx polymers (D30-D100).

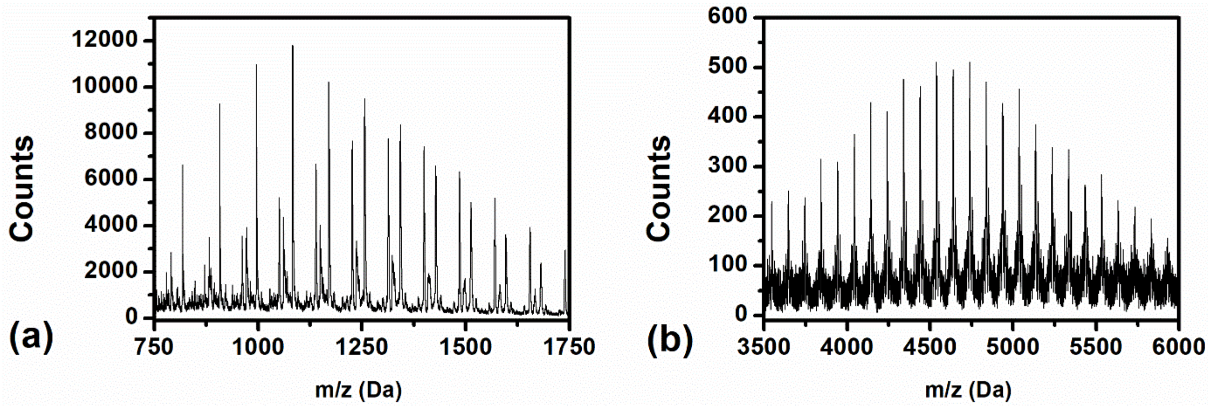

Figure S5. MALDI-TOF-MS of: (a) A10 and (b) A50, respectively.

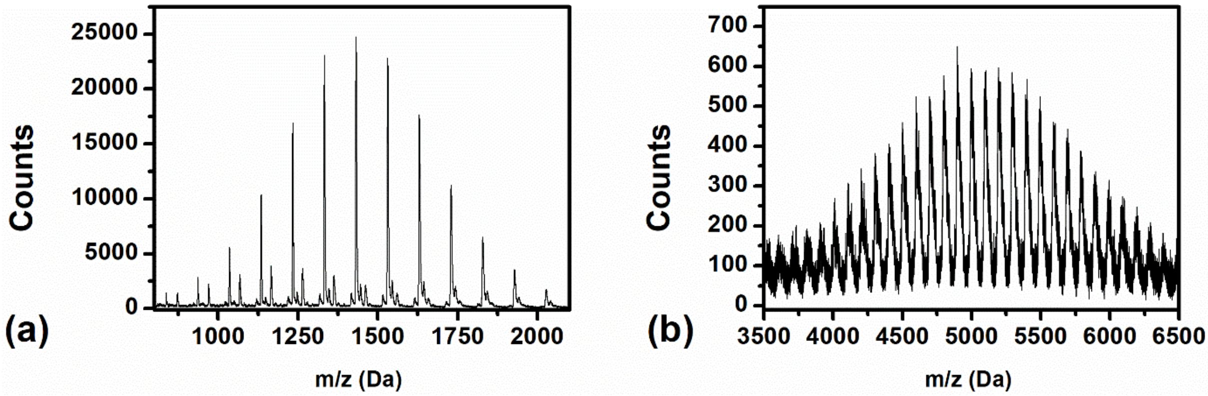

Figure S6. MALDI-TOF-MS of: (a) D10 and (b) D50, respectively.

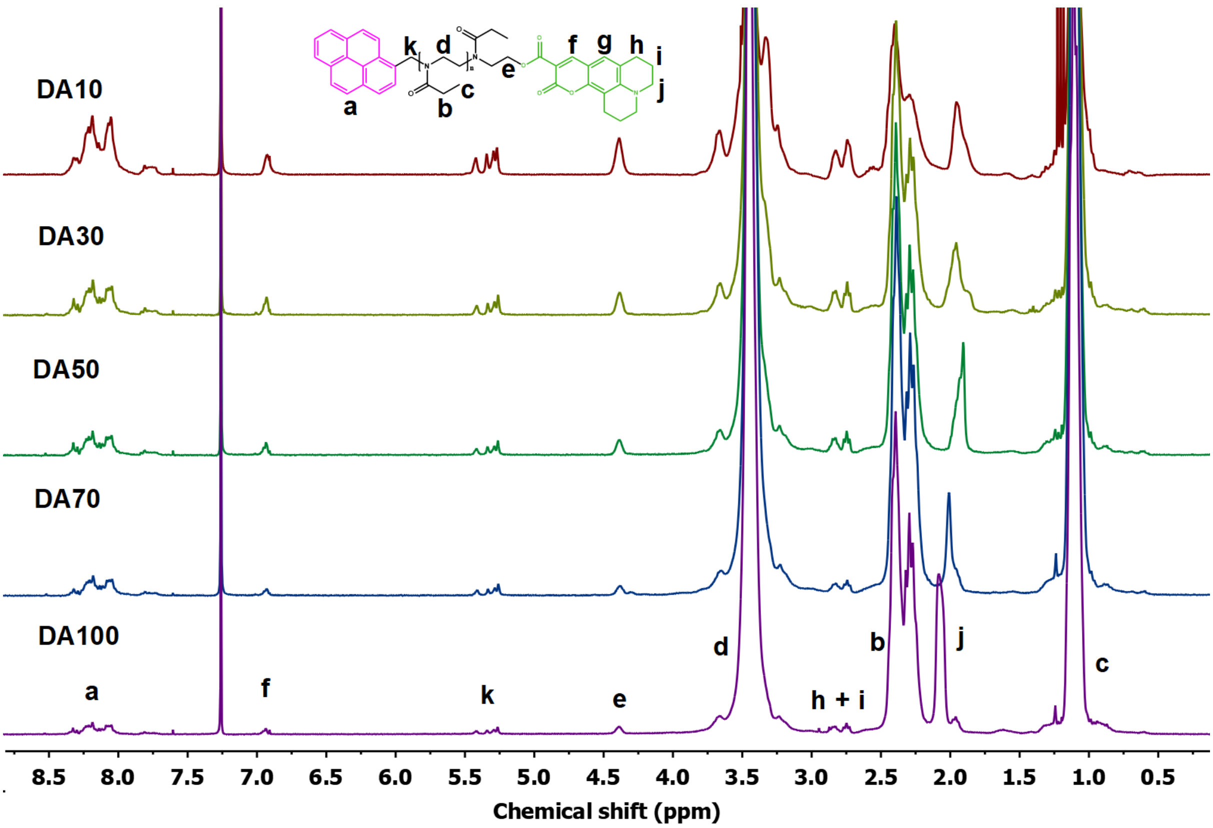

Figure S7. ^{1}H-NMR spectra of dual labeled PEtOx polymers (DA10-DA100).

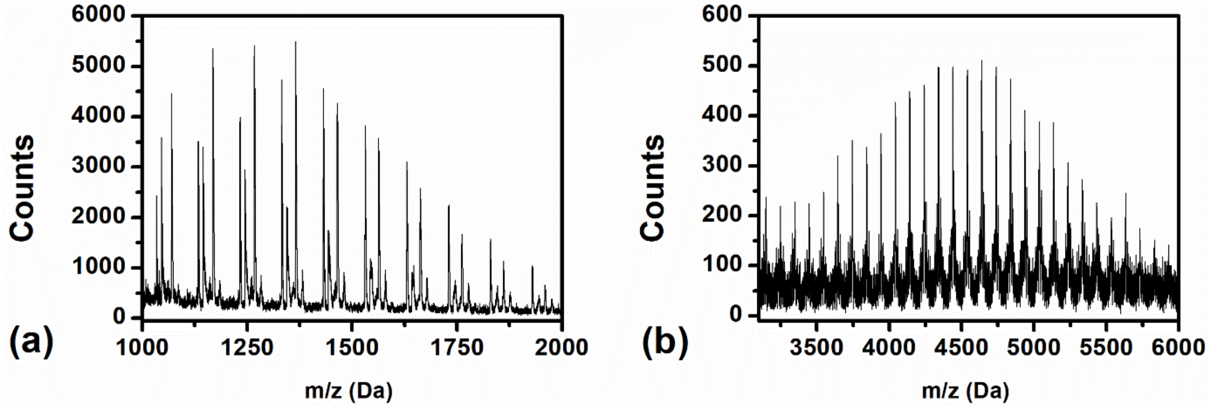

Figure S8. MALDI-TOF-MS of: (a) DA10 and (b) DA50, respectively.

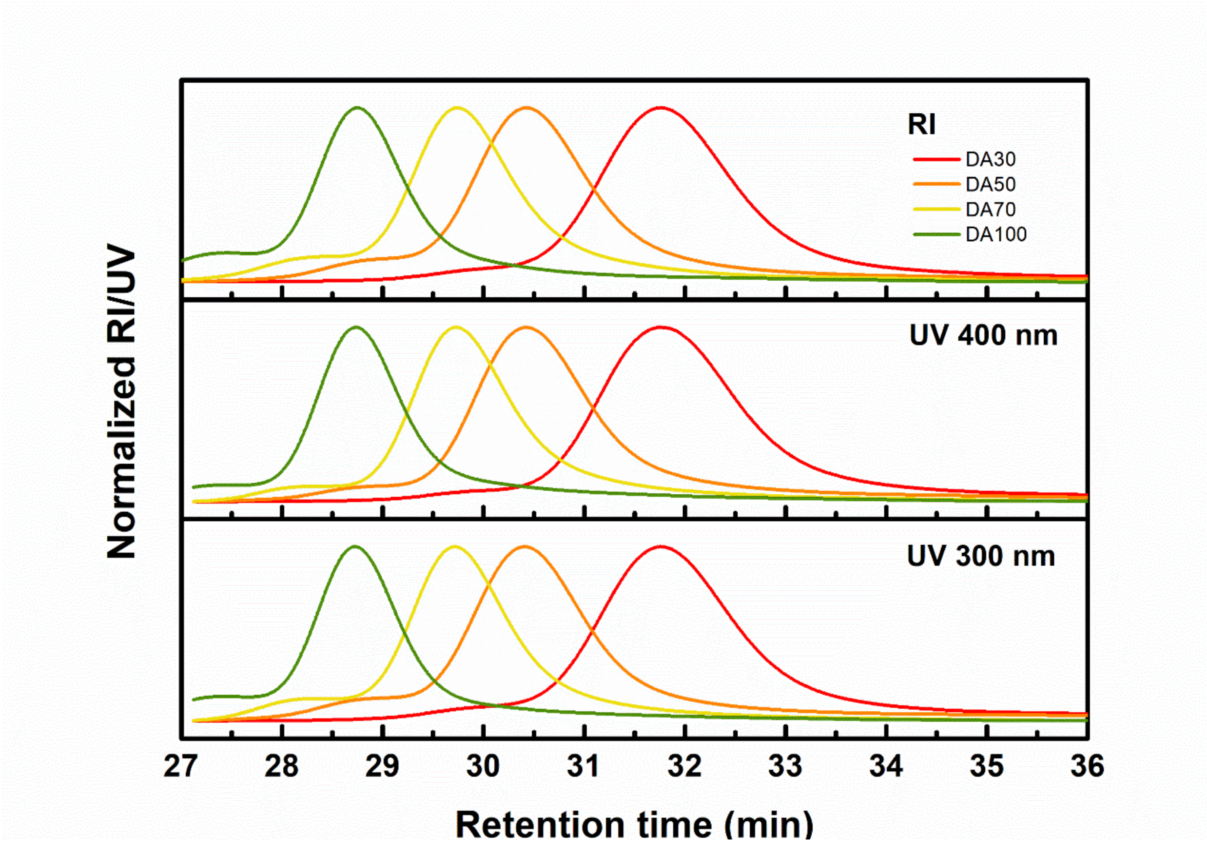

Figure S9. Normalized SEC-RI (top) and SEC UV (bottom) traces of dual labeled PEtOx polymers (DA30-DA100).

Table S1. Structural characterization of α-Py labeled PEtOx polymers.

Polymer code	Yield (%)	DP[a]	Mn (Da)[b]	Mn (Da)[c]	Đ[b]	T_{CP} (°C)[d]	Φ ($CHCl_3$)	Φ (H_2O)
iD10	72	10	2000	1063	1.05	n.s.	0.17	0.48
iD30	95	30	6000	2953	1.09	50.2	0.19	0.56
iD50	92	50	9500	5152	1.09	56.7	0.26	0.57
iD70	89	70	13600	7043	1.12	55.6	0.32	0.69
iD100	88	100	14000	10782	1.13	55.7	0.42	0.67

[a]Theoretical degree of polymerization.
[b]Determined from DMA SEC using PMMA calibration.
[c]Determined from MALDI-TOF.
[d]Cloud point temperature in deionized water (10 mg/mL; 0.5°C/min)

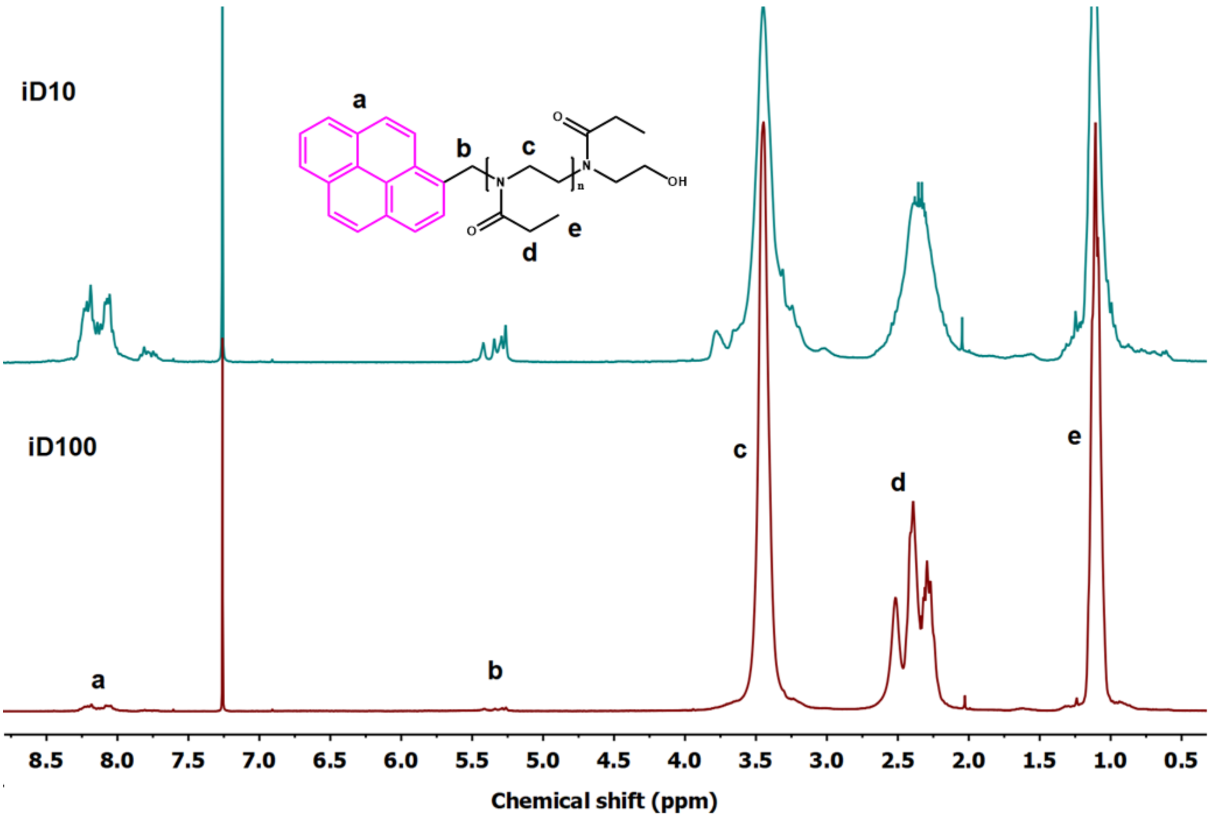

Figure S10. ^{1}H-NMR spectra of α-Py single labeled PEtOx polymers (iD10 and iD100).

S2: Photophysical characterization of single and dual fluorescent dye labeled PEtOx polymers

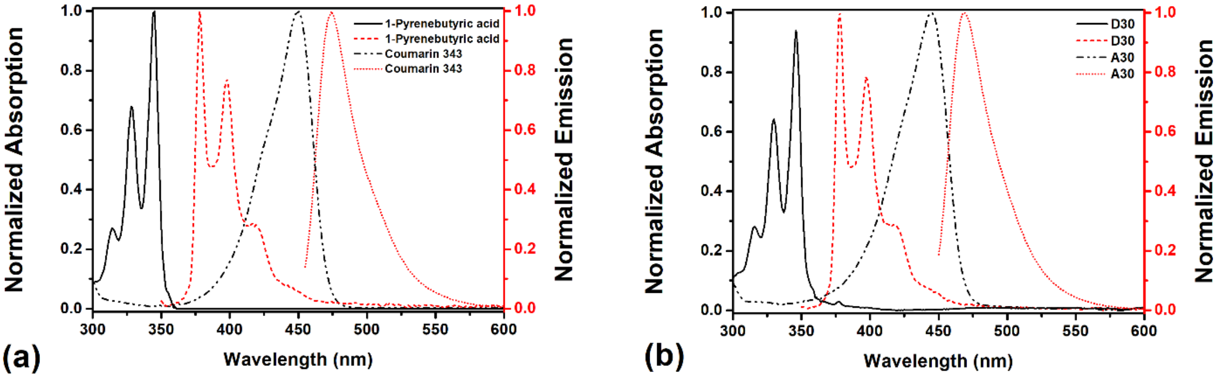

Figure S11. Absorption and emission spectra of: (a) 1-pyrenebutyric acid, and coumarin 343; and (b) PEtOx single labeled polymers (D30 and A30), respectively. The excitation wavelength was 345 nm and 445 nm for Py and Cou343, respectively.

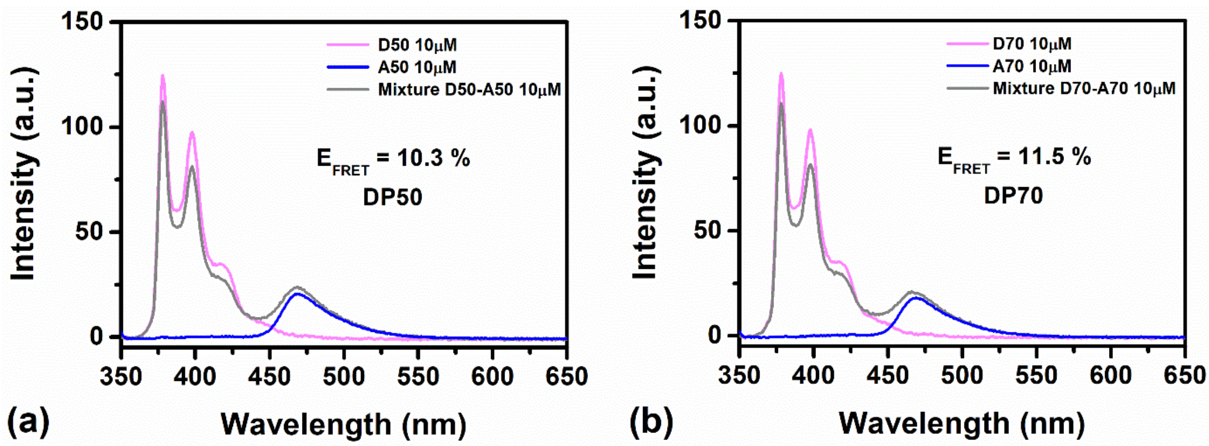

Figure S12. Emission spectra of: (a) D50, A50 and equimolar mixture of D50 and A50 in $CHCl_3$, and (b) D700, A70 and equimolar mixture of D70 and A70 in $CHCl_3$. In all cases excitation wavelength was 345 nm and the concentration was 10μM.

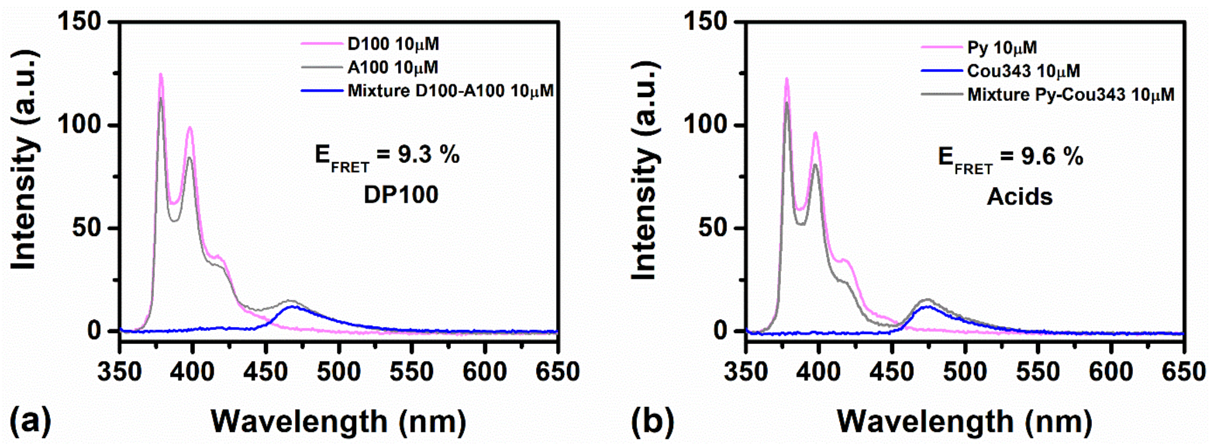

Figure S13. Emission spectra of: (a) D100, A100 and equimolar mixture of D100 and A100 in $CHCl_3$, and (b) 1-pyrenebutyric acid (Py), Coumarin 343 (Cou 343) and equimolar mixture of Py and Cou 343 in $CHCl_3$. In all cases excitation wavelength was 345 nm and the concentration was 10μM.

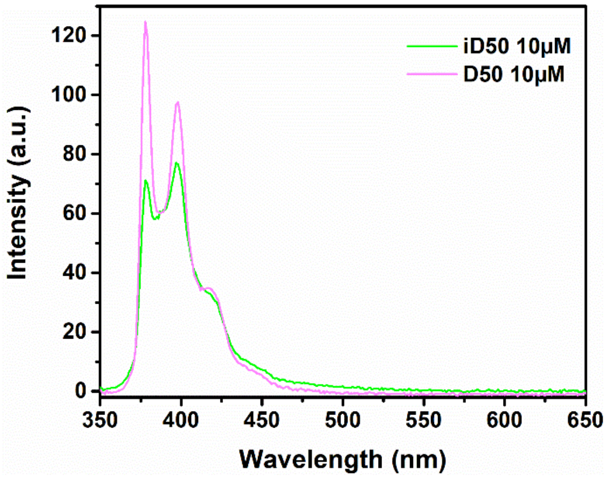

Figure S14. Emission spectra of α-Py labeled PEtOx (iD50) and ω- Py labeled PEtOx (D50) having a DP of 50 in $CHCl_3$. In all cases excitation wavelength was 345 nm and the concentration was 10μM.

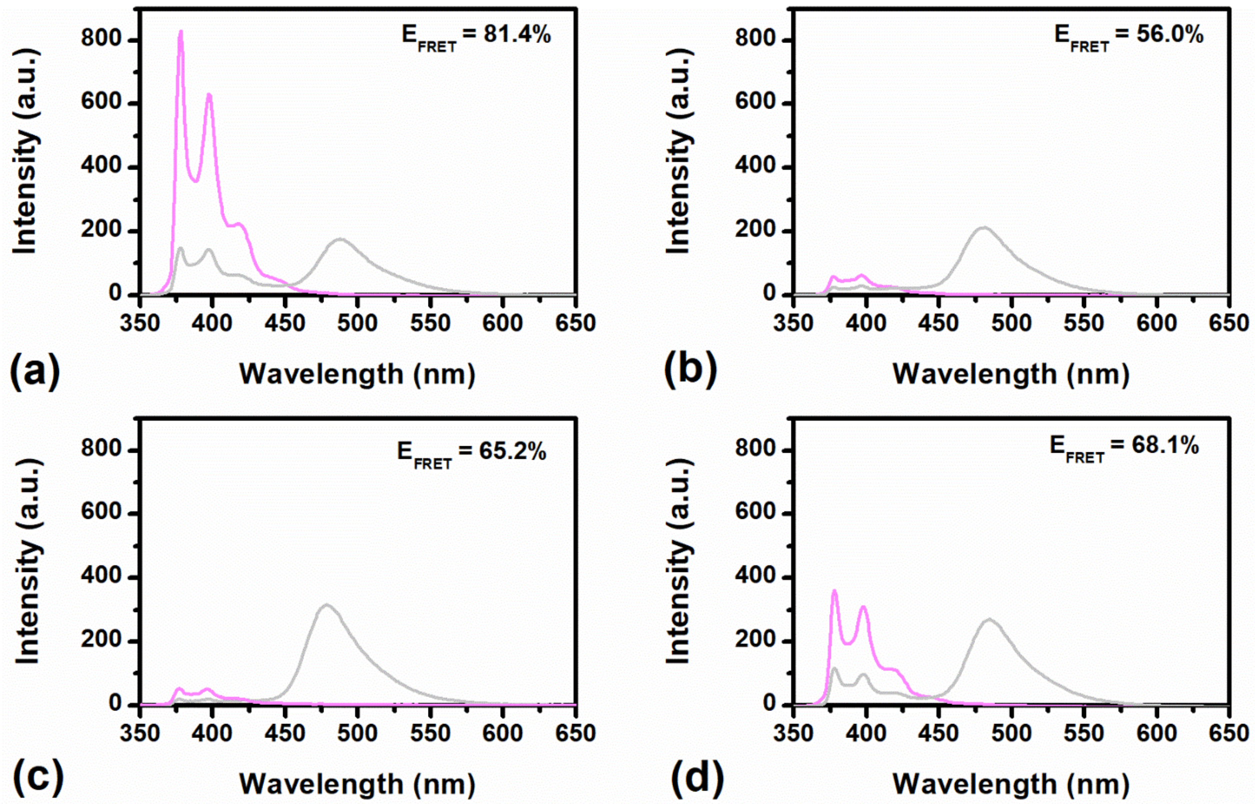

Figure S15. Emission spectra of α-Py single labeled (iD30) polymers and dual labeled (DA30) polymers in different solvents: (a) ethylene glycol, (b) ethanol, (c) acetonitrile, and (d) dimethyl sulfoxide. In all cases, excitation wavelength was 345 nm and the concentration was 10μM.

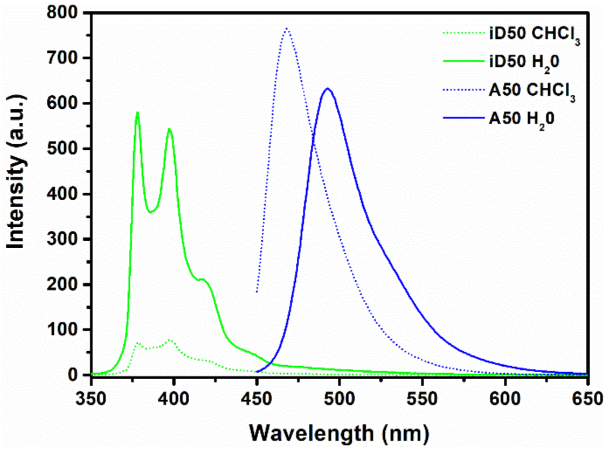

Figure S16. Emission spectra of α-Py labeled PEtOx (iD50) and ω- Cou343 labeled PEtOx (A50) having a DP of 50 in $CHCl_3$ and H_2O. In all cases the fluorophore concentration was 10µM and the excitation wavelength was 345 nm and 445 nm for iD50 and A50, respectively.

Quantum yield Calculations

Solutions of pyrene containing polymers were analyzed to determine the quantum yield of the dye in both water and chloroform. The gradients of these polymers were compared to the gradient of the anthracene standard. The raw data for DP10 in H_2O are shown in Figure S17, while the plot of absorbance vs fluorescence intensity is given in Figure S18.

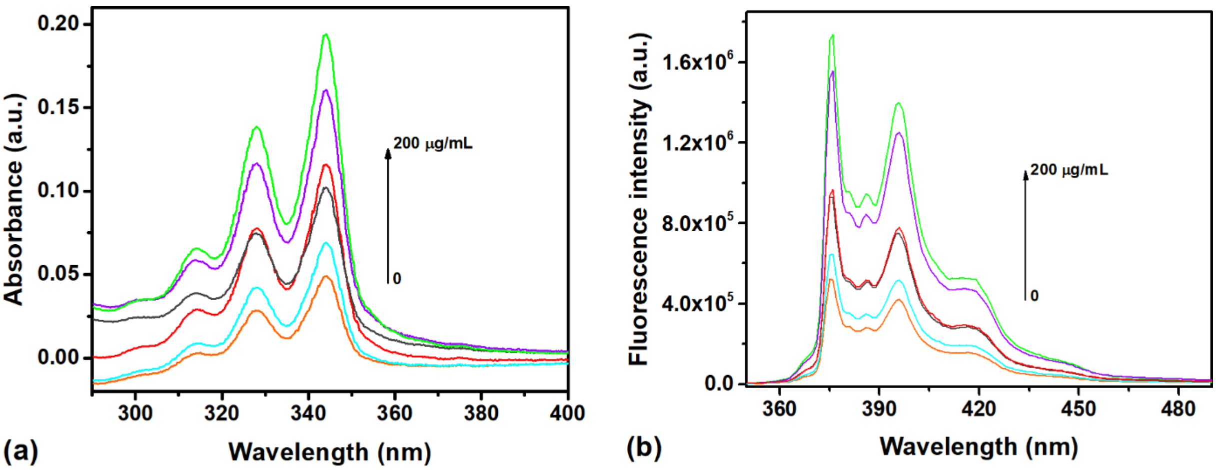

Figure S17. (a) Absorption, and (b) fluorescence emission spectra of iD10 in H_2O at various concentrations between 0 -200 µg ml^{-1}.

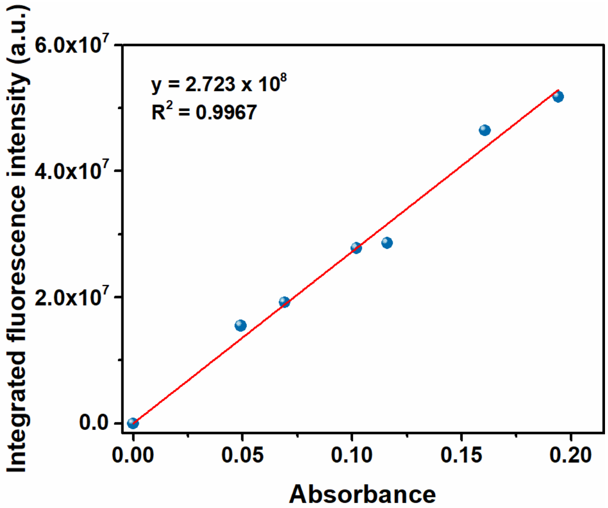

Figure S18. Linear plots of absorbance vs integrated fluorescence emission for iD10 in water. The gradient of the sample is equal to the slope of the line.

S3: DOSY NMR characterization single and dual fluorescent dye labeled PEtOx polymers

The polymer hydrodynamic radii (R_H) were determined by analysis of DOSY spectra to determine the diffusion coefficient of both the PEtOx chains and the solvent. Typical processed data (using Bruker Topspin 3.5) is shown below in Figure S19 where the distinct diffusions of both the polymer backbone and solvent can be observed.

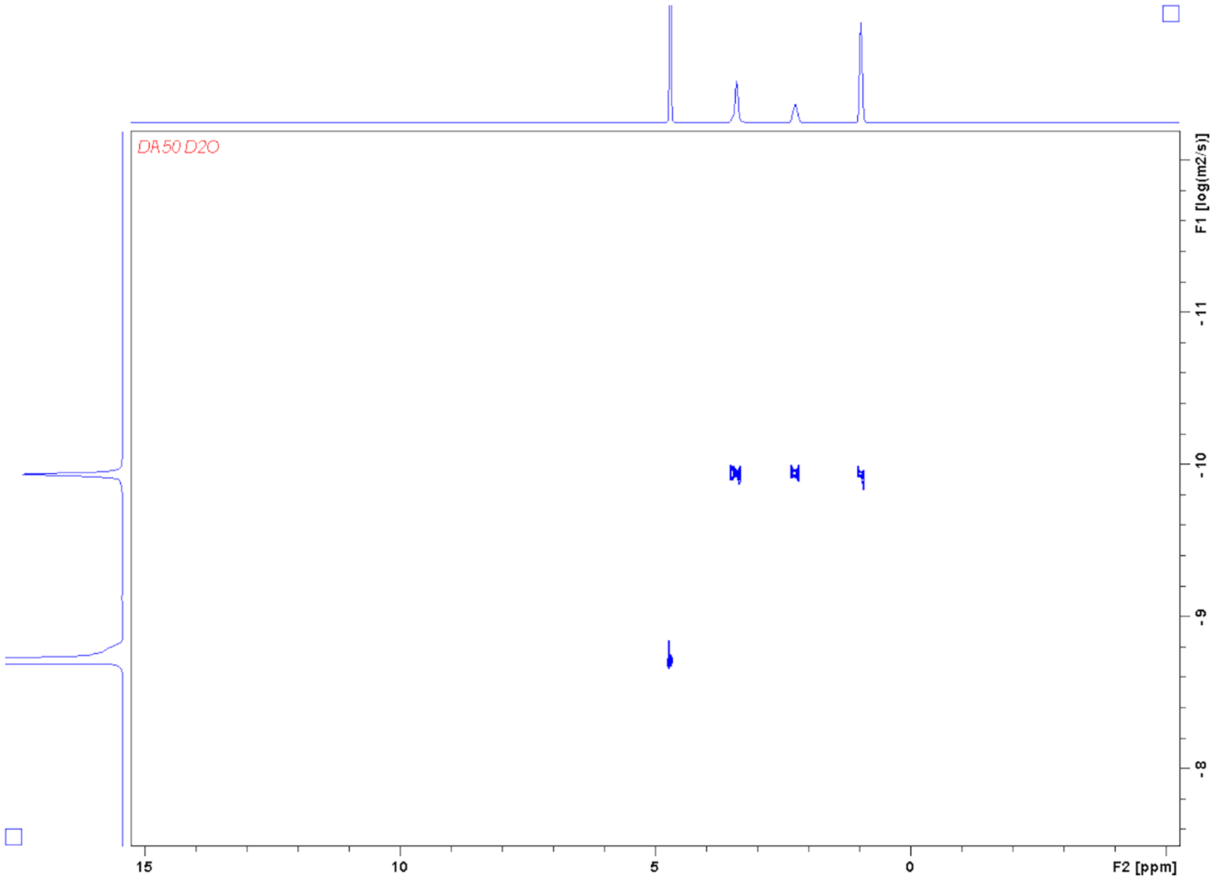

Figure S19. Screenshot of processed DOSY data for DA50 in D_2O showing distinct polymer diffusion (-9.946 log m^2 s^{-1}) and solvent diffusion (-8.701 log m^2 s^{-1})

Accurate diffusion properties for all samples were plotted and converted into hydrodynamic radii that are shown in Table S2. This measurement of solvated single chain radii is comparable to the smaller peak observed in DLS sizing data although this also indicates the presence of larger aggregates even below the LCST (Figure S20).

Table S2. Calculated hydrodynamic radii (in nm) of single fluorophore labeled PEtOx in $CDCl_3$ and D_2O, respectively.

Polymer code	iD10	iD30	iD50	iD70	iD100	A10	A30	A50	A70	A100
$R_{H, CHCl3}$ (nm)	4.43	4.13	6.51	6.26	11.08	2.42	5.58	5.09	6.24	6.77
$R_{H, H2O}$ (nm)	12.45	15.57	19.55	22.92	27.49	11.28	16.00	20.01	22.71	27.43

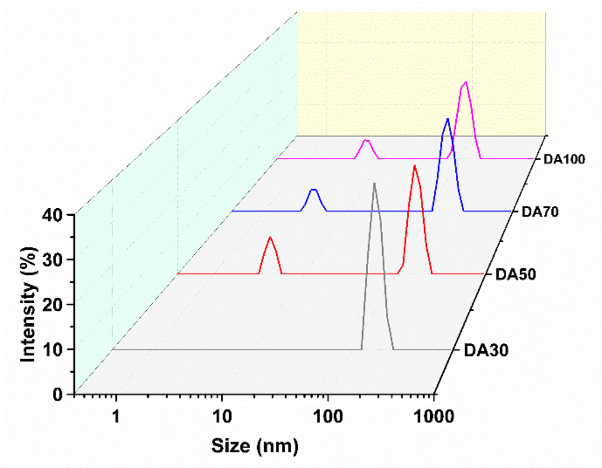

Figure S20. Dynamic Light Scattering (DLS) data for a 1 mg·mL^{-1} aqueous solution of DA10-100 polymers at 25 °C.

S4: Thermoresponsive behavior of single and dual fluorescent dye labeled PEtOx polymers

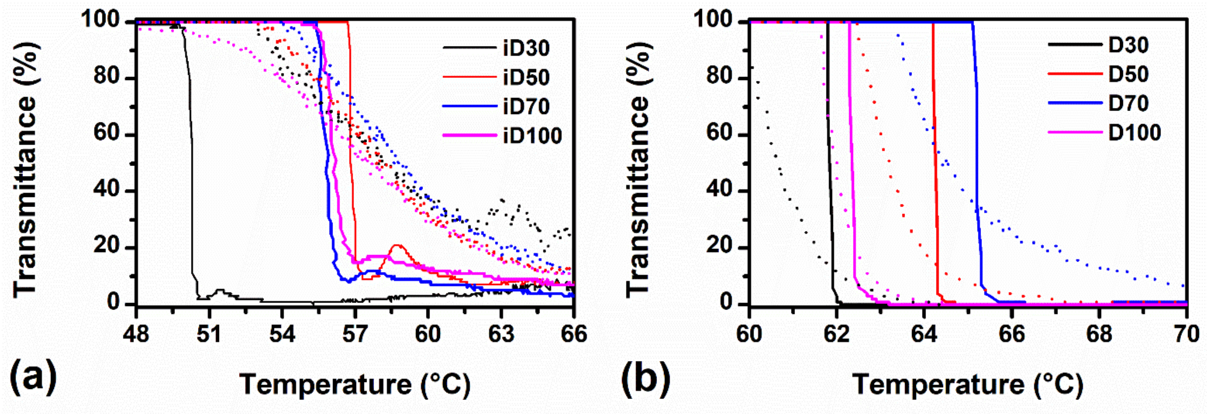

Figure S21. Transmittance versus temperature profiles for the second heating (solid lines) and cooling (dashed lines) cycles of iD and D series in deionized water (10 mg ml^{-1}; 0.5 °C min^{-1}).

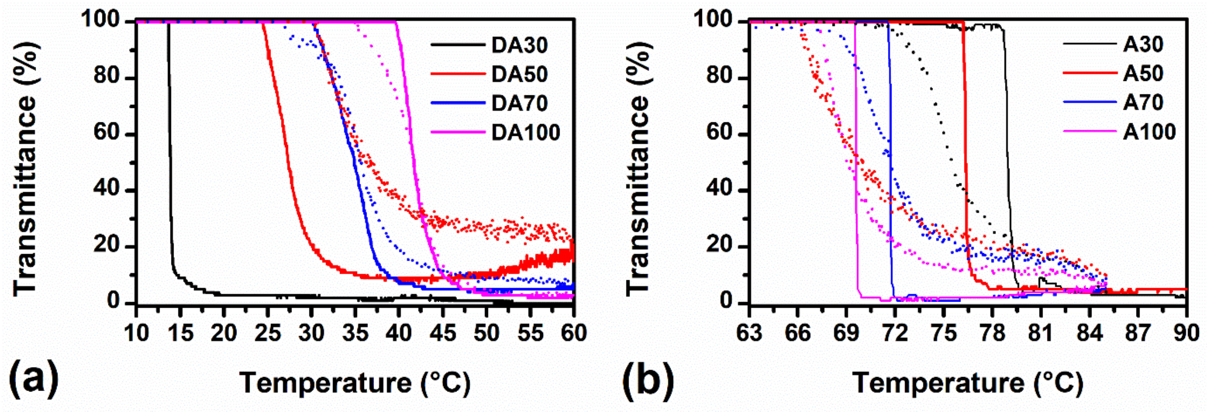

Figure S22. Transmittance versus temperature profiles for the second heating (solid lines) and cooling (dashed lines) cycles of A and DA series in deionized water (10 mg ml^{-1}; 0.5 °C min^{-1}).

S5: Time correlated simple photon counting measurements

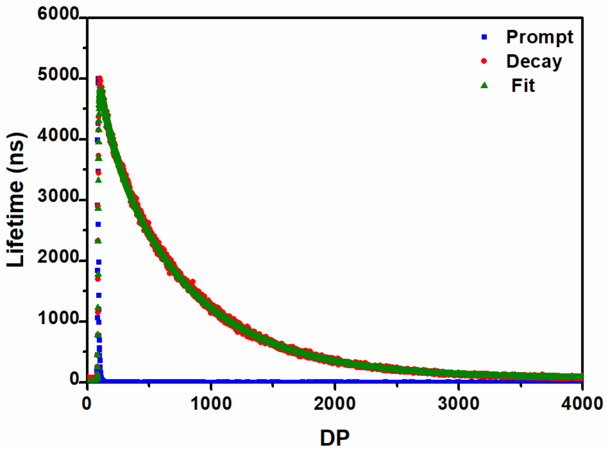

Figure S23. Example raw decay, and fitted lifetime, of iD30 fluorescent emission at 410 nm. Blue data indicates scattering from a silica prompt at the excitation source wavelength.

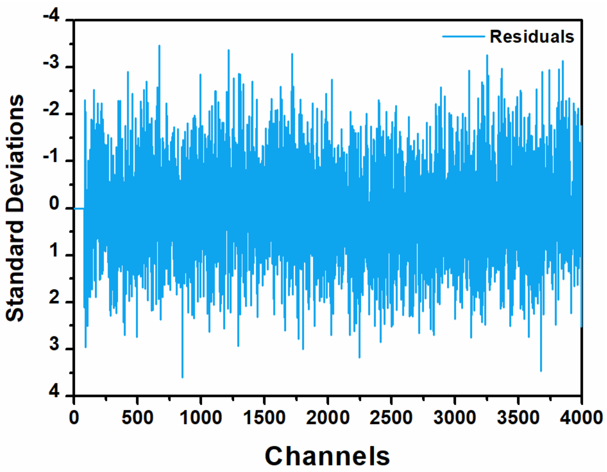

Figure S24. Example residual standard deviations of the fitted dual exponential lifetime (iD-30).

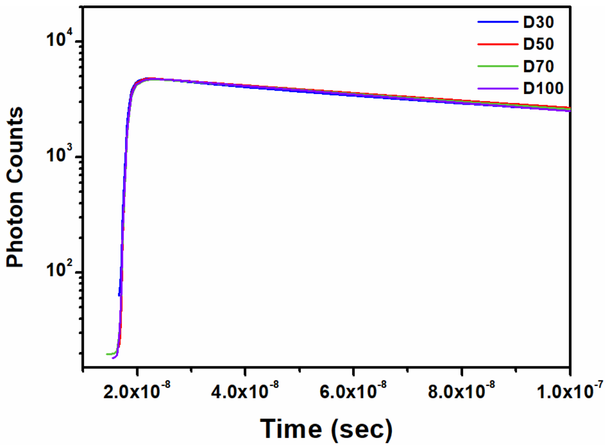

Figure S25. Fitted decays of donor polymer series (iD30 to iD100) after 345 nm excitation at 410 nm emission.

Table S3. Full profiles of lifetime fitting process using equation 1 for pyrene excitation in the D and DA polymer series.

Polymer code	**$\tau_{average}$ (ns)**	**$SD_{\tau average}$ (ns)[a]**	**τ_1 (s)**	**$SD_{\tau 1}$ (s)[a]**	**τ_2 (s)**	**$SD_{\tau 2}$ (s)[a]**	**B**	**α_1**	**α_2**	**ChiSq**
iD10	-	-	-	-	-	-	-	-	-	-
iD30	143.0	0.77	2.54 E-08	1.28 E-09	1.47 E-07	2.01 E-10	6.25 E+01	1.69 E-02	9.61 E-02	1.06
iD50	143.1	2.07	4.44 E-08	3.31 E-09	1.46 E-07	2.21 E-10	2.26 E+01	1.01 E-02	1.02 E-01	1.01
iD70	139.7	2.63	5.45 E-08	3.72 E-09	1.45 E-07	2.61 E-10	1.96 E+01	1.38 E-02	9.08 E-02	1.01
iD100	132.9	2.20	5.74 E-08	2.97 E-09	1.40 E-07	2.88 E-10	1.83 E+01	2.08 E-02	8.55 E-02	1.06
DA10	90.4	0.25	1.32 E-09	2.02 E-11	1.29 E-07	5.89 E-10	3.49 E+00	2.60 E-01	6.03 E-03	1.29
DA30	99.0	0.41	1.96 E-09	3.21 E-11	1.23 E-07	6.95 E-10	5.09 E+01	1.82 E-01	1.10 E-02	1.77
DA50	77.8	0.31	2.48 E-09	4.92 E-11	9.43 E-08	5.20 E-10	1.92 E+02	1.50 E-01	1.81 E-02	1.88
DA70	93.9	0.24	2.08 E-09	3.39 E-11	1.09 E-07	4.01 E-10	2.37 E+01	1.67 E-01	1.86 E-02	1.95
DA100	111.7	0.18	1.66 E-09	2.43 E-11	1.22 E-07	2.82 E-10	1.26 E+01	1.86 E-01	2.65 E-02	1.55

[a]SD represents the standard deviation

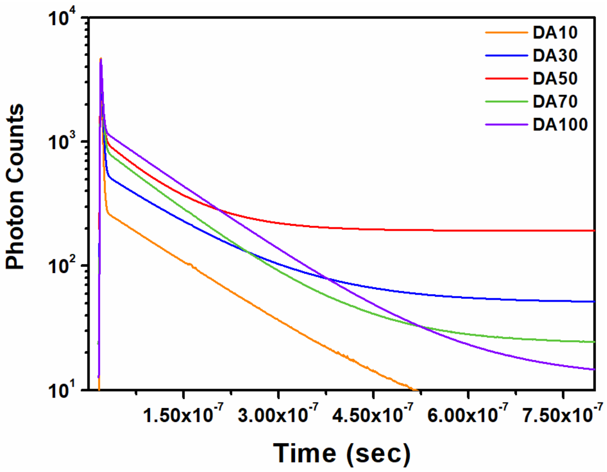

Figure S26. Fitted decays of donor-acceptor polymer series (DA10 to DA100) after 345 nm excitation and 550 nm emission.

Table S4. Full profiles of lifetime fitting process using equation 1 for coumarin 343 excitation in the A and DA polymers series.

Polymer code	$\tau_{average}$ (ns)	SD$\tau_{average}$ (ns)[a]	τ_1 (s)	SDτ_1 (s)[a]	τ_2 (s)	SDτ_2 (s)[a]	B	α_1	α_2	ChiSq
A10	-	-	-	-	-	-	-	-		-
A30	7.3	0.23	3.49 E-09	1.68 E-10	6.05 E-09	2.99 E-11	4.88 E+00	-2.0 E-01	3.48 E-01	1.33
A50	6.3	0.07	3.24 E-09	8.78 E-11	5.85 E-09	3.27 E-11	2.30 E+00	- 5.40 E-02	2.22 E-01	1.10
A70	5.8	0.028	3.02 E-09	6.65 E-11	5.64 E-09	3.42 E-11	0.68 E+00	- 1.70 E-02	1.97 E-01	1.10
A100	5.1	0.88	4.87 E-09	8.88 E-10	8.43 E-09	7.38 E-10	6.72 E-02	1.78 E-01	5.99 E-03	1.06
DA10	4.7	0.127	3.71 E-09	1.37 E-10	6.03 E-09	9.32 E-11	3.35 E-01	1.34 E-01	5.87 E-02	0.89
DA30	7.8	0.047	3.97 E-09	1.56 E-10	7.78 E-09	4.97 E-11	1.05 E+01	-1.2 E-03	1.72 E-01	1.15
DA50	7.0	0.058	3.59 E-09	8.76 E-11	7.45 E-09	4.43 E-11	9.58 E+00	5.21 E-02	2.13 E-01	1.16
DA70	5.2	0.131	4.07 E-09	1.40 E-10	6.89 E-09	1.01 E-10	1.68 E+00	1.37 E-01	5.14 E-02	0.85
DA100	4.8	0.196	3.40 E-09	2.26 E-10	5.85 E-09	7.28 E-11	0.38 E-01	0.11 0016	8.15 E-02	1.11

[a]SD represents the standard deviation

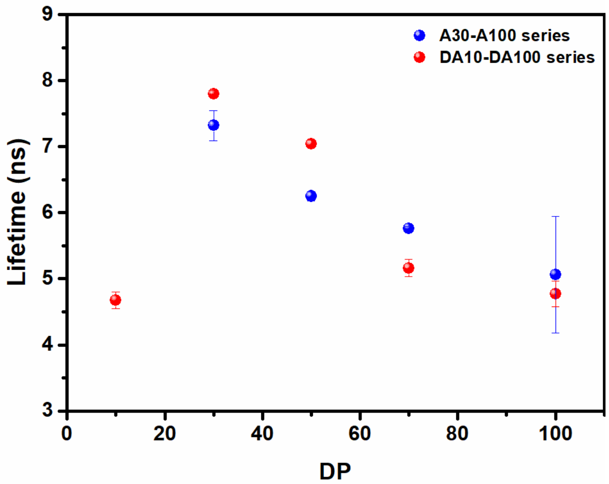

Figure S27. Fluorescence lifetime of coumarine 343 moiety in A30-100 and DA10-100 polymer series following excitation at 430 nm. In all cases the polymer concetration was 1 mg·ml^{-1}.

S6: Thermoresponsive FRET behavior

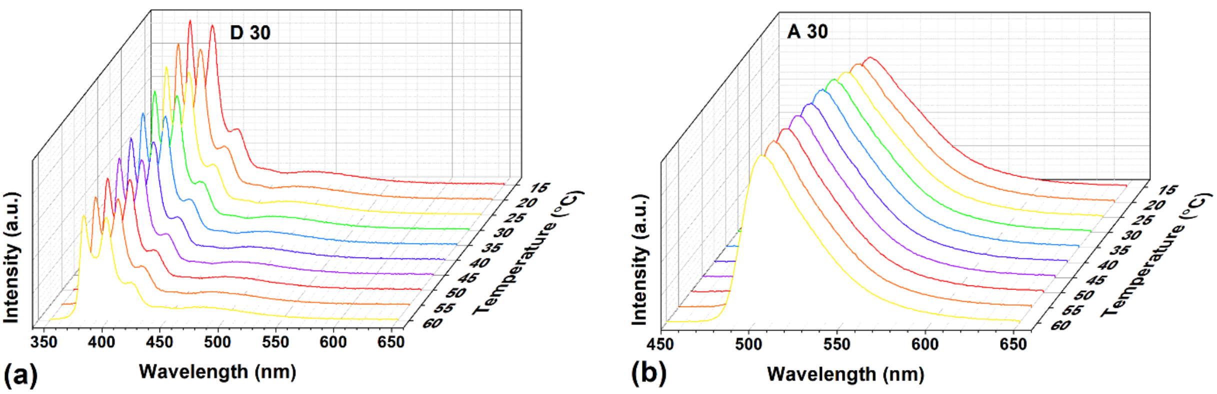

Figure S28. Fluorescence spectra as a function of temperature for (a) D30, and (b) A30, respectively. In all cases the polymer concentration was 1 mg·mL^{-1} and the excitation wavelength was 345 nm and 445 nm for D30 and A30, respectively.

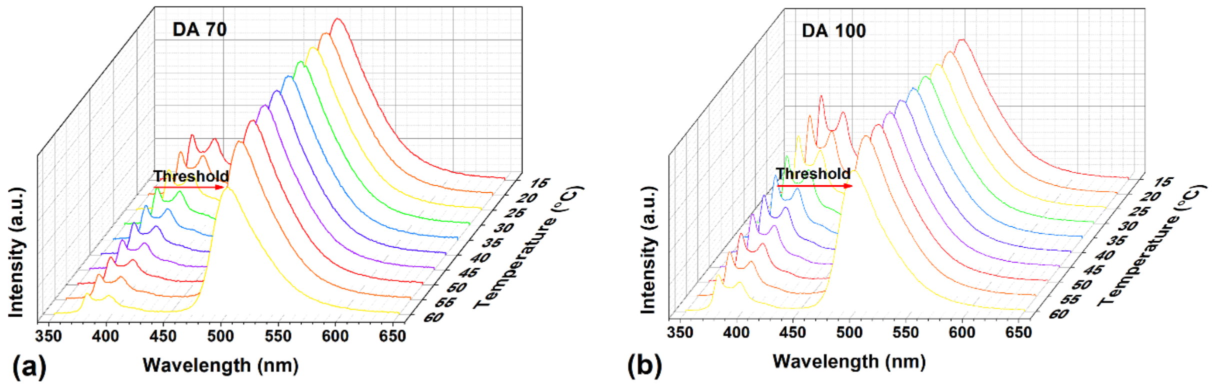

Figure S29. Fluorescence spectra as a function of temperature for (a) DA70, and (b) DA100, respectively. In all cases excitation wavelength was 345 nm and the concentration of the polymer was 1 mg·mL^{-1}.

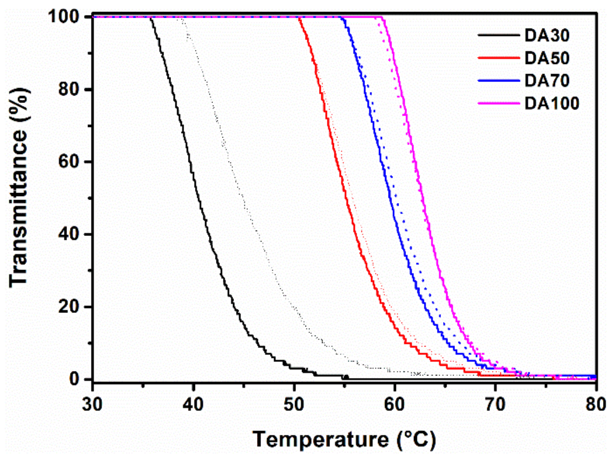

Figure S30. Transmittance versus temperature profiles for the second heating (solid lines) and cooling (dashed lines) cycles of DA series in deionized water (1 mg ml^{-1}; 0.5 °C min^{-1}).

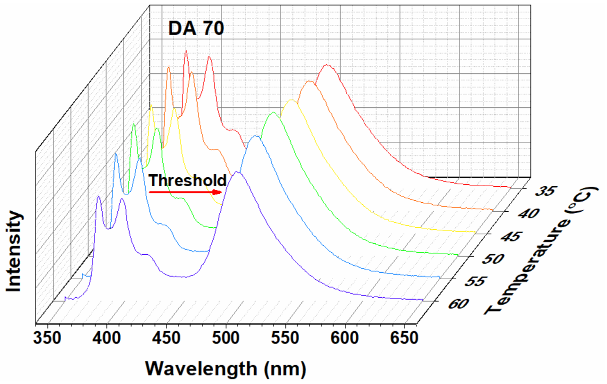

Figure S31. Fluorescence spectra as a function of temperature for DA70. The excitation wavelength was 345 nm and the concentration of the polymer was 0.1 mg·mL^{-1}.

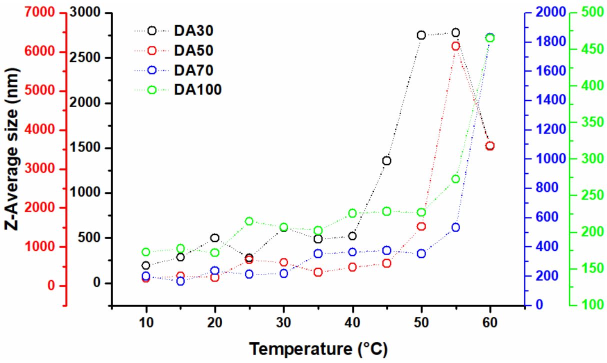

Figure S32. Z-average size versus temperature of DA30-100 series in deionized water (1 mg·mL^{-1}) determined by DLS. Lines were added to guide the eyes.

S7: FRET behavior in the solid state

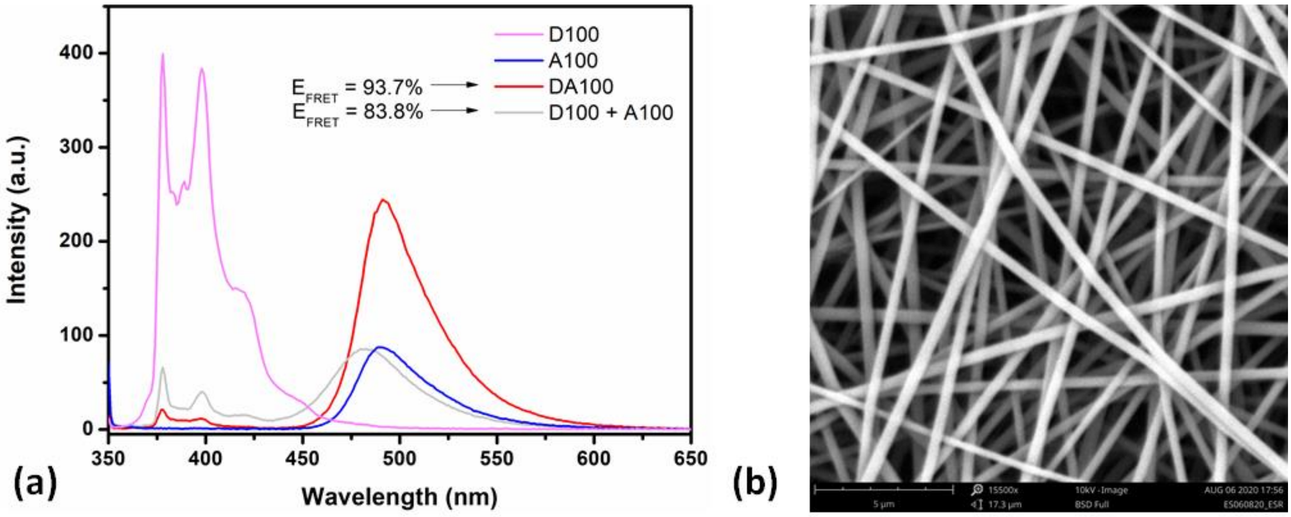

Figure S33. (a) Emission spectra of D100, A100, mixture of D100+A100 and DA100 nanofibers; (b) SEM image of the mixture of D100 +A100 nanofibers.